Obtaining new composite biomaterials by means of mineralization of methacrylate hydrogels using the reaction-diffusion method

Yousof Ramadan[1], M. Isabel González-Sánchez[2], Karl Hawkins[3], Jorge Rubio-Retama[1], Edelmira Valero[2], Stefano Perni[4,6], Polina Prokopovich[4,5,6], Enrique López-Cabarcos[1]

[1]*Department of Physical Chemistry II, Faculty of Pharmacy, Complutense University of Madrid, 28040 Madrid, Spain*

[2]*Department of Physical Chemistry, School of Industrial Engineering, Castilla-La Mancha University, 02071 Albacete, Spain*

[3]*Centre of Nanohealth, Institute of Life Sciences, College of Medicine, Swansea University, Singleton Park, Swansea SA2 8PP, Wales, UK*

[4]*School of Pharmacy and Pharmaceutical Sciences, Cardiff University, Cardiff CF103NB, UK*

[5]*Institute of Medical Engineering and Medical Physics, School of Engineering, Cardiff University, Cardiff, UK*

[6] *Department of Biological Engineering, Massachusetts Institute of Technology, Cambridge, USA*

Corresponding author: Enrique López-Cabarcos[1]

cabarcos@farm.ucm.es

Abstract

The present paper describes the synthesis and characterization of a new polymeric biomaterial mineralized with calcium phosphate using the reaction-diffusion method. The scaffold of this biomaterial was a hydrogel constituted by biocompatible polyethylene glycol methyl ether methacrylate (PEGMEM) and 2-(dimethylamino)ethyl methacrylate (DMAEM), which were cross-linked with N-N'-methylenebisacrylamide (BIS). The cross-linking content of the hydrogels was varied from 0.25% to 15% (w/w). The gels were used as matrix where two reactants (Na_2HPO_4 and $CaCl_2$) diffused from both ends of the gel and upon encountering produced calcium phosphate crystals that precipitated within the polymer matrix forming bands. The shape of the crystals was tuned by modifying the matrix porosity in such a way that when the polymer matrix was slightly reticulated the diffusion reaction produced round calcium phosphate microcrystals, whilst when the polymer matrix was highly reticulated the reaction yielded flat calcium phosphate crystals. Selected area electron diffraction performed on the nanocrystals that constitute the microcrystals showed that they were formed by Brushite ($CaHPO_4.2H_2O$). This new composite material could be useful in medical and dentistry applications such as bone regeneration, bone repair or tissue engineering.

Keywords: composite materials, reaction diffusion, brushite particles, hydrogels, bone regeneration material.

Introduction

The study of the precipitate formation within a gel after the encounter of two reaction fronts that diffuse from opposite sides enables to relate scientific fields that are normally separated such as gel structure, progress of reaction fronts, crystal growth in gels, nanoparticles synthesis, simulation of nonlinear phenomena, etc. This is an old research subject and during most of the early period, the main interest was held by the phenomenon of Liesegang rings; however, more recently a new approach was taken in the context of order formation out of chaos and simulation of the process [1-5]. For several decades mineralization of an organic matrix has been an important topic in bone-tissue engineering [6]. There are numerous reports about mineralization, for example, through immersion in simulated body fluid [7] or an alternate soaking process [8] and a natural diffusion process through a biopolymer membrane [9]. However, these methods form 2D mineralised surfaces on the biomaterial, which is not useful in bone repair and osseoregeneration processes. As 3D mineralization was observed in the hydrogels, very recently they started been used as a good model to study this process, in consequence that many mineralization processes take place in gelling environments [10-12]. Most of the research in this

field was performed using physical gels such as gelatin, agarose, silica, starch, polyvinyl alcohol) hydrogels [2, 13, 14]whilst only few studies were conducted with chemical gels [15].

The integration of micro- or/and nano- size particles in synthetic hydrogels can be a way to create new biomaterials. One difficulty lies in getting a homogeneous distribution of the inorganic particles across the organic matrix and in controlling their composition and crystal size. Hydrogels have been associated with some biomineralization systems [10] such as: tooth enamel in mammals [16], nacreous layer in mollusk shells [17] and trout otoliths [18]; therefore, hydrogels could provide the matrix to grow inorganic calcium phosphate particles. Organic matrixes made of cross-linked hydrogels based on methacrylates have been proven non cytotoxic, non-immunoreactive and their porosity could be controlled by the amount of cross-linker used in their synthesis [19]. Furthermore, lately, hydrogels based on methacrylates have been used as tissue expanders before vertical ridge augmentation to facilitate the wound closure and to prevent the exposure of the bone grafts to the oral cavity demonstrating the possible applications of these materials in dentistry [20].

It has been previously shown that a new biomaterial could developed combining the cohesion provided by the gel with the bone regeneration properties of calcium phosphate particles [21-23]. In this work, we have prepared a new copolymer hydrogel composed of two well known and widely used methacrylate polymers [24-28] containing calcium phosphate nanoparticles. The particle formation within the gel was achieved through a reaction diffusion process:

$$Na_2HPO4 + CaCl_2 + 2H_2O \rightarrow \quad CaHPO_4 \cdot 2H_2O + 2ClNa$$

Electrolyte solutions of sodium hydrogen phosphate and calcium chloride were allowed to diffuse from opposite sides of the gel; the low solubility of calcium phosphate resulted in the precipitation of nanoparticles when saturation was reached. The properties of the inorganic nanoparticles formed within the gel, as well as the physical properties of the gels, were studied in this work. The growth of calcium phosphate particles in methacrylate hydrogels constituted, a new biomaterial which could have potential benefits in dentistry and orthopaedic tissue regeneration.

Materials and methods

Chemicals

The monomers polyethylene glycol methyl ether methacrylate (PEGMEM), and 2-dimethylamino ethyl methacrylate (DMAEM), and the cross linker *N*,*N*′-methylenebis(acrylamide) (BIS) were purchased from Sigma Aldrich. The initiator ammonium

persulfate (APS) was purchased from Fluka. $Na_2HPO_4 \cdot 2 \cdot H_2O$ (DHP) and $CaCl_2$ were purchased from Panreac.

Synthesis of the gel

The gels were prepared by adding 2 ml of PEGMEM (0.0065 mol) and 1 ml of DMAEM (0.0065 mol) to 5 ml deionised water at room temperature. Subsequently, appropriate amounts of BIS and APS were added under stirring, finally the mixture was allowed to polymerize for 25 minutes. During the polymerization the temperature was recorded every 30 seconds. After preparation, the gels were dialyzed against milliQ water at room temperature for two weeks to remove the unreacted monomers and oligomers.

Two groups of gels were prepared as described above: i) initiator content was varied between 1 mg/mL and 7 mg/mL and no crosslinker was used in the preparation of the gels; ii) crosslinker concentration varied between 0.25 % and 15 % (w/w) whereas the concentration of initiator was kept at 1 mg/mL.

Reaction diffusion experiments

A piece of the swelled gel was inserted in the middle of a PTF tube (1.5 cm in diameter and 7 cm in length) and connected to both sides with silicone tubes of 54 cm length and 8mm diameter, that connected both sides with two bottles of 200 ml that served as reservoirs for Ca (solution of 20 mM) and phosphate (solution of 20 mM). The formation and evolution of the calcium phosphate precipitate was followed every day using a Canon RE-650 video recorder. The pictures obtained were analyzed using Image J to measure the lengths of the gel, the width of the calcium phosphate precipitate formed in the gel and the position of the centre of the band; for the latter purpose the border of the gel from which the solution of $CaCl_2$ diffuses was assumed as origin for the position measurements. The experimental setup and a scheme of the experiment are shown in Figure 1.

Gel Characterization Methods

The chemical composition of the gel was studied using FTIR (Thermo Nicolet IR200) covering the wave number range between 500 and 3500 cm^{-1}. Bruker Avance 250 MHz ^1H NMR was used to investigate the ratio of both monomers used in the synthesis in the final gel The decomposition temperature and water content of the gel were measured with DSC Mettler 820 equipped with a cooler operated by liquid Nitrogen; the samples were heated at a rate of 5^oC/min. The characterization of the calcium phosphate precipitate formed on the surface of the gel by reaction diffusion method was carried out by scanning electron microscope (SEM) JSM 6335F (JEOL) operated at 10 and 20 kV. In addition, transmission electron microscope (TEM) JEM 1010 (JEOL) working at 100 kV was used to image the calcium phosphate particles as well as selected area electron diffraction patterns. The samples examined by TEM were

prepared in a similar way as biological samples; the gel was embedded in resin for 48 to 72 hours at 60 °C, then a microtome was used to cut thin slices (100 nm thick) that were ready for use.

Gel swelling behaviour

The gels were immersed completely in deionised water and they were weighted daily. The hydration of the gel was obtained according to Eq. 1.

$$H = \frac{(m_f - m_i)}{m_i} \quad (1)$$

where m_i and m_f are the weights of the gel before and after swelling respectively.

The effect of NaCl solutions with different concentration in swelling process was also investigated. For these experiments pieces of a fully swollen gel (2.5% cross-linking) were placed in NaCl solutions with salt concentrations of 1, 2.5, 5, 10, 15, 20, 25, 30% (w/w) till equilibrium was reached (around 2 days).

Rheological properties of gels

The gel was loaded into the rheometer (The ARES-G2 Rheometer (TA Instruments), for each rheological test, approximately 3g of gel were used and the experiment was performed at 37°C. The serrated parallel plates (to prevent slippage) to sandwich the material at a constant but low normal force were employed. G' was monitored as the material equilibrates and as the gap reduces. When G' becomes constant, it was assumed that the material is appropriately in contact with the plates and the frequency sweep (0.01 to 10 Hz). All measurements were conducted at a strain of 0.1 %, which was within the linear viscoelastic range of the material, as confirmed by a strain sweep and the absence of a third harmonic response

Results and discussion

Gel characterization

The research scope of this work was to develop new biomaterials based on hydrogels reinforced with calcium phosphate particles for their application in bone regeneration. Controlling temperature during gel formation is very important especially if the gel is planned to be used as matrix for the immobilization of drugs, proteins or thermolabile molecules that could be destroyed during the polymerization. For this reason, we investigated the evolution of temperature, as function of time, for gels prepared with the concentration of PEGMEM and DMAEM given before, without crosslinker, but with different amounts of initiator; the results are presented in Figure 2. In all cases, the maximum temperature reached during the polymerization reaction was between 32 and 38 ºC.

It is known that light is scattered by fluctuations in density and concentration within the gel, that is the deviation of the density and concentration from their average value in the sample. Thus, light is scattered only when its wavelength is greater than the size of the dishomogeneities within the gel, conversely, the light will be reflected if its wavelength is smaller. Gels prepared with a concentration of APS higher than 2 mg/mL were not transparent indicating lack of homogeneity in the material, additionally the polymerization temperature in these gels reached values above 35 ºC (Figure 2) which is too high to allow the entrapment of biomolecules or drugs. Thus, all subsequent experiments in this work were carried out using the concentration of initiator of 1 mg/ml, as it produced transparent gels (data not shown), the temperature did not exceed 34 ºC and the gelling process took around 30 minutes.

^{1}H NMR spectrum was recorded for a gel with no cross-linking agent to determine the ratio between monomers in the produced copolymer gel (Figure 3). The M_W of the PEGMEM used was 300 g/mol and that means an average of 4 PEG units in each PEGMEM molecule. It is known that the peak between 3.4 and 3.6 ppm corresponds to the PEG polymer units [29] and, therefore, this peak roughly correspond to 18 H atoms. It is also known that the peak at 4.2 is associated with the protons attached to the ester group. By integrating this later peak and referring the area to the previous peak, we calculated that it corresponded to 4 H atoms. Since the ester group is presented in both polymers, i.e., each polymer shared 2 H atoms; we deduced that the ratio of the polymer in the copolymer was 1:1 which is consistent with the equimolar amount of monomers used in the synthesis of the copolymer.

An important property of chemical gels is that they can absorb a considerable amount of water; this effect has to be considered when studying the formation of precipitates within them. The concentration of cross-linker controls the swelling behaviour and porosity of the gel, therefore, we prepared gels whose content of crosslinking was varied between 0.25% and 15% (molar ratio) to investigate its effect on the swelling behaviour of the copolymer gels. For this purpose, they were immersed completely in deionised water and the relative increase in weight of the gels was measured as function of time (Figure 4a). The gel slowly swelled reaching equilibrium after around 9 days. For the gel with 0.25% cross linking $m_f > 20m_i$ after 9 days, whereas the gel with 15% cross linking reached the swelling equilibrium after 6 days when $m_f > 2m_i$ (Figure 4a).

The thermodynamic description of swelling in gels is given by the Gibbs free energy and its variation, ΔG, resulting from the mixing a polymer network with a solvent. Thus, the swelling thermodynamics can be interpreted in terms of osmotic pressure $\Pi = - (\delta G/\delta V)_T$. Polymer networks play the role of an osmotic membrane through which the osmotic pressure acts. At $\Pi = 0$ the gel is at equilibrium with the outer solvent molecules and there is no transfer of solvent across the gel-solvent interface. However, $\Pi > 0$ causes the network swelling as water

penetrates the gel, on the contrary, for $\Pi < 0$, the gel collapses and the water moves from inside to outside the gel (de-swelling phenomenon).

We were able to withdraw most of the water taken by the gel during the swelling process using NaCl solutions. In **Error! Reference source not found.**b the relative weight loss as function of the ionic strength ($I = 1/2\sum z_j^2 \cdot m_j$ with z_j the ion charge and m_j the ion molality) is presented. If the gel was introduced in a solution of 25 % (w/w) salt (I = 4.27 mol/L), the gel lost most of the water that had acquired during the swelling process and returned to its initial dimensions.

The gels were further analyzed by differential scanning calorimetry (DSC). The thermogram of a 25% crosslinked gel is presented in Figure 5a; it shows a shifting of the melting temperature of the water and the presence of two evaporation peaks at around 100 and 120 ºC, thus indicating the presence of different types of water within the gel. In the inset of Figure 5a can also be seen that the onset of gel decomposition occurred at around 280 ºC. This gel with high cross linking agent concentration was used for the determination of the decomposition temperature because temperature values for gels with lower concentration of cross linking agent were not as clear as in this case due to the high water content of such gels.

There are three types of water in hydrogels [22-24], namely: i) non-freezing water which is bound to the polymer chains and does not exhibit phase transition, ii) free water that freezes/melts similarly to pure water and iii) freezing bound water which interacts weakly with the polymer chains freezing/melting at temperatures slightly shifted with respect to pure water. With the aim of investigating the different types of water present in our gels we performed thermograms as function of the crosslinking content of the gels (see Figure5b).

The fraction of the freezing water (X_f, free water and freezing bound water) within the hydrogel can be calculated from the area under the corresponding endothermic peak (ΔH_{endo}) (see **Error! Reference source not found.**b) according to Eq. 2:

$$X_f(\%) = \frac{\Delta H_{endo}}{\Delta H_w} \cdot 100 \quad (2)$$

where ΔH_w = 333, 3 J/g is the heat of fusion of pure water.

Then, the amount of non-freezing bound water (W_{nf}) can be calculated as:

$$W_{nf=} W_\infty - W_f \quad (2)$$

where W_∞ is the equilibrium water content of the hydrogel and can be calculated according to Eq. 3:

$$W_\infty(\%) = \frac{ESD}{ESD+1} \cdot 100 \quad (3)$$

ESD is the equilibrium swelling degree that represents the amount of water per each gram of dry gel and can be calculated by the next equation:

$$ESD\left(\frac{g_{water}}{g_{dry\ polymer}}\right) = \frac{m_{f-}(m_i-5)}{(m_i-5)} \quad (4)$$

where m_f and m_i were defined in Eq. 1.

The 5 ml of water used during the gelling process were subtracted from the initial weight of the gel (m_i) to get the actual value of the dry gel.

Recently, the influence of the PEG molecular weight upon the state of water in PEG-ethylenediamine hydrogels was investigated and it was found that the amount of freezing water depends mostly on the structure and size of the meshes of the polymer network and varies between 54 and 74% depending on the hydrogel composition [24]. On the other hand, the non-freezing water content depends on the chemical structure of the gel. Here, we investigated the influence of crosslinking concentration on the percentage of freezing and non-freezing water within the microgel and the results obtained are presented in Table 1. It can be seen that the amount of freezing water decreased, whilst the proportion of non-freezing water increased as the crosslinking content of the gels increased. This tendency may be explained by a large number of water molecules binding the PEGMEM/DMAEM chains through hydrogen bonds with the carboxylate groups in the polymer chains.

The rheological properties of gels as function of the cross-linking agent percentage are shown in Figure 6; The elastic modulus (*G'*) did not change with frequency for all gels, however, its value was dependent on the percentage of the cross linking (Figure 6a). When 1% of cross linking agent was employed, *G'* was 2500 Pa, this increased to 84000 Pa when 7% was added. Conversely, *G"* did show a decreasing behaviour with increasing frequency Figure 6b; nevertheless, even at the lowest frequency tested in this work (1 Hz), the value of *G"* was nearly a tenth of the value of *G'*.

Mineralization of the gels

The control of the nucleation and growth of calcium phosphate crystals within biocompatible hydrogels has regenerated interest in the last few years after the discovery that hydrogels with functionalized organic surfaces can control crystal morphology and orientation [6]; it was also a recent finding that calcite single crystals can incorporate macromolecules [7]; finally, the interest of using gels in three-dimensional biomimetic mineralization [25]. Figure 7 shows a temporal sequence of the formation of precipitates within the PEGMEM/DMAEM gel using the reaction-diffusion method. This method may contribute to the preparation of calcium phosphate

particles with controlled size and specific composition, depending on the reactants used as well as the porosity of the matrix employed in the synthesis of the crystals.

Figure 7 shows images of the gels taken during several days after the beginning of the reaction. It has been reported that when the reactants diffuse from both sides of the gel, in case they have similar diffusion coefficients, the precipitates appear preferentially in the central part of the gel [5]. Since we used equal concentrations for both reagents (20 mM) and the diffusion coefficients of hydrated ions in water at infinite dilution are similar ($D_{HPO4\ 2-} = 7.6.\cdot 10^{-10}$ m^2/s and $D_{Ca2+} = 7.9 \cdot 10^{-10}$ m^2/s) [29], we observed that the precipitates began to appear close to the gel centre. However, as time passed, the band widened towards the edge through which the calcium ions flowed (Figure 8a) and slightly moved away from the edge through which the phosphate ions flowed. This behaviour occurred in all the gels, independently of their cross-linking content (Figure 8a). It is worth mentioning that the band of precipitates appeared in the region where the two reaction fronts encounter and in this case no Liesegang bands are formed.

In the gel with 7% cross-linking and 1.6 cm length, the band of precipitates begined to appear after 4 hours and 20 minutes at a distance of 0.72 cm from the gel edge through which the calcium ions flowed and 0.88 cm from the gel edge through which the phosphate ions flowed (Figure 7 and Figure 8a). We can estimate the diffusion coefficient of both ions from the following equation:

$$h = \sqrt{6Dt} \tag{5}$$

where:

h is the distance travelled by the ions in cm

t is the time in seconds

D is the diffusion coefficient

Thus, we obtained $D_{HPO4} = 8.3\ 10^{-10}$ m^2/s and $D_{Ca2+} = 5.5\ 10^{-10}$ m^2/s. Even though the percentage of error is high because the exact time of formation of a band is not well defined, it seems that the diffusion coefficient of the HPO_4^{2-} ions approached its value at infinite dilution closer than the diffusion coefficient of Ca^{2+} ions. In addition, the band grew towards the side where the calcium flowed and these two observations seems to indicate that the interaction of the Ca^{2+} ions with the polymer network is stronger than the interactions of the HPO_4^{2-} ions.

Most of the physical gels maintain their size during the formation of precipitates. Conversely, the size of the PEGMEM/DMAEM gels increased when the cross-linking content decreases as is shown in Figure 8b. This result can be understood in light of results presented in Figure 4b that showed the ionic strength control of the gel swelling properties. During the formation of precipitates the ionic strength within the gel should decrease and consequently the gel swelled.

Figure 8b shows the evolution of the width of the band as a function of time for the two gels investigated. The width of the band grows conspicuously during the first 6 - 7 days and then levels off for longer times. The width of the band formed in the 2.5 % cross-linked gels was larger than the one formed in the 7% cross-linked gels.

When the calcium phosphate precipitates reached the end of the gel at Ca^{2+} solution side, the experiment was stopped and the gel-calcium phosphate composite was freeze dried for 5 days and prepared for SEM examination. Figure 9 shows a micrograph of the freeze dried 2.5 % cross-linked microgel at low magnification (x20). The composite material consists of layers of polymer in which the calcium phosphate precipitates are attached.

To further investigate the nature of the precipitate particles we performed SEM on two cuts taken from two different locations, one on the surface of the material and the other in the central part of the gel. Figure 10 summarised the results obtained as a function of the cross-linking content. For gels prepared with 0.5% cross-linking, the surface was covered with well defined calcium phosphate particles with sizes smaller than 1 micron, whereas in the inner part of the gel the formation of aggregates was predominant (Figure 10). As the cross-linking content increased, the surface of the gel started to be covered by plates of precipitates, whilst in the inner part there were still rounded shape particles (sample with 1% cross-linking) but for gels with 5% cross-linking the plates appeared not only on the surface but also in the central part of the gel (Figure 10).

The rounded well distributed particles appeared under the TEM microscope as aggregates of smaller particles with a length of around 100 nm and with needle shape (Figure 11) or in some cases as nanotubes organized in chains that can be seen in the same figure.

In order to determine what type of calcium phosphate was precipitated, we performed X-ray diffraction of the samples. However, the X-Ray diffraction pattern showed no crystalline peaks and only two broad amorphous halos that can be distinguished at around $2\theta = 30\ ^\circ$ and $65\ ^\circ$ respectively.

However, if we selected some of the nanotubes that can be seen in Figure 11 and perform selected area electron diffraction (SAED), we could determin they were crystals. The nanocrystals in Figure12a and b showed a clear diffraction pattern, whereas when they aggregated, forming a round particle, the orientation of crystals in all directions resulted in broad halos, as is illustrated in Figure 12c. The d-spacing (Table 2) can be calculated using the following modified Bragg equation:

$$L\lambda = DR \tag{6}$$

Where:

L is the distance between the sample and the detector

λ is the wavelength of the electron beam

R is the radius of the diffraction peak.

. Comparing the d-spacing values obtained from SAED pattern to the well known d-spacing values of different calcium phosphates, we concluded that all the peaks were to be attributed to $CaHPO_4 \cdot 2H_2O$, so the crystals were made of Brushite (see Table 2).

Conclusions

We have synthesized chemical gels based on copolymers of biocompatible PEG methyl ether methacrylate and 2-(dimethylamino)ethyl methacrylate with different cross-linking content (between 0.25% and 15%). We have demonstrated that, by adjusting the cross-linking and the ionic strength, we can control the swelling and de-swelling behaviour of the gels.

Using Na_2HPO_4 and $CaCl_2$ as reagents, we were able to produce a composite material with inorganic particles and/or inorganic plates homogeneously distributed forming a band of precipitates within the gel. The width and the position of the band depended on the concentration of the reactants and the cross-linking content of the gel. The precipitates were formed by round particles that became plates when the cross-linking content of the gel increased. Selected electron diffraction performed on the nanocrystals that constituted the round particles showed that the precipitates were mainly formed by brushite. The gel itself, or the composite material with the brushite particles integrated within the gel, might be used as bone regeneration material in orthopedic applications, bone tissue engineering and also as drug delivery system.

Acknowledgments

The authors acknowledge financial support from the Spanish Science and Innovation Ministry (Grant MAT2010-15349), from the Regional Ministry of Science and Technology (Consejería de Ciencia y Tecnología; JCCM, Spain) (POII-10-0235-8597) and from COST Action CM1101. PP also thanks Arthritis Research UK (ARUK:18461) for the financial support.

References

1.- H.K. Henisch. *Crystals in Gels and Liesegang Rings*, Cambridge University Press, (1988), New York, USA

2.- E.Karpati-Smidroczki, A.Buki, M. Zrinyl, Colloid Polymer Sci. (1995) 273, 857-865. *Pattern forming precipitation in gels due to coupling of chemical reactions with diffusion.*

3.- S. Kai, S.C.Muller, J.Ross. J. Chem. Phys. (1982), 76, 1392. *Measurements of temporal and spatial sequences of events in periodic precipitation processes*

4.- B. Chopard, P. Luthi, M. Droz. Phys. Rev. Lett. (1994) 72, 1384. *Reaction-diffusion cellular automata model for the formation of Leisegang patterns.*

5.- E. Lopez Cabarcos, Chein-Shiu kuo, A. Scala, R. Bansil., Phys. Rev. Lett. (1996) 77, 2834–2837. *Crossover between Spatially Confined Precipitation and Periodic Pattern Formation in Reaction Diffusion System.*

6. - S. Mann. Biomineralization: *Principles and concepts in bioinorganic materials chemistry.* Oxford university press: New York, 2001.

7. - W. L. Murphy, D.J.J. Mooney. J. Am. Chem. Soc. 2002, 124: 1910-1917. *Bioinspired growth of crystalline carbonate apatite on biodegradable polymer substrata.*

8. - J. Watanabe, M. Alashi, Biomacromolecules (2007) 8, 2288-2293. *Formation of hydroxyapatite provides a tunable protein reservoir within porous polyester membranes by an improved soaking process.*

9. - S.H. Teng, J.J. Shi, L.J. Chen, J. Colloids Sup. B. (2006) 49, 87-92, *Formation of calcium phosphates in gelatin with a novel diffusion system.*

10.- Hanying Li, Lara. A. Estroff. J. Am. Chem. Soc. (2007) 129, 5480-5483. *Hydrogels Coupled with Self-assembled Monolayers. An in Vivo Matrix to Study Calcite Biomineralization.*

11.- Hanying Li, Huolin L.Xin, David A. Muller, Lara. A. Estroff. Science (2009) 326, 1244-1277. *Visualizing the 3D Internal structure of Calcite Single Crystals Grown in Agarose Hydrogels.*

12.-L. Silverman, A.L. Boskey. Calcif. Tissue Int. (2004) 75 (6), 494-501. *Diffusion Systems for Evalution of Biomineralization.*

13- C.G. Sander, C. Leeuwenburgh, ‚Junichiro Jo, Huanan Wang, Masaya Yamamoto, John A. Jansen, and Yasuhiko Tabata. *Biomacromolecules* (2010), 11*,* 2653–2659, *Mineralization, Biodegradation, and Drug Release Behavior of Gelatin/Apatite Composite Microspheres for Bone Regeneration.*

14- J. Sohier, P. Corre, P. Weiss, P. Layrolle, Acta Biomaterialia 6 (2010) 2932–2939, *Hydrogel/calcium phosphate composites require specific properties for three-dimensional culture of human bone mesenchymal cells.*

15- Taishi Yokoi, Masakazu Kawashita, Koichi Kikuta, Chikara Ohtsuki. Materials Science and Engineering C (2010) 30, 154–159, *Biomimetic mineralization of calcium phosphate crystals in polyacrylamide hydrogel: Effect of concentrations of calcium and phosphate ions on crystalline phases and morphology.*

16. - J. Moradian-Oldak. J. Matrix Biol. (2001) 20, 293-305. *Amelogenins: assembly, processing and control of crystal morphology.*

17. - Y. Levi-Kalisman, G. Falini, L. Addadi, S.J. Weiner. J. Struct. Biol. (2001) 135, 8-17. *Structure of the nacreous organic matrix of a bivalve mollusk shell examined in the hydrated state using Cryo-TEM.*

18. - E. Murayama, Y. Takagi, T. Ohira, J.G. Davis, M.I. Greene, H. Nagasawa. Eur. J. Biochem. (2002) 269, 688-696. *Fish otolith contains a unique structural protein, otolin-1.*

19.-S. Van Vlierberghe, P. Dubruel, E.Schacht. Biomacromolecules (2011) 12, 1387-1408. *Biopolymer-Based Hydrogels as Scaffolds for Tissue Engineering Applications: A Review.*

20.- Dogan Kaner, Anton Friedmann. J. Clin.periodontol. (2011) 38(1), 95-101. *Soft tissue expansion with self-filling osmotic tissue expanders before vertical ridge augmentation: a proof of principle study.*

21.- Faleh Tamimi, Jesus Torres, Carlos Kathan, Rafael Baca, Celia Clemente, Luis Blanco, Enrique Lopez Cabarcos. J. Biomed. Mat. Res. Part A (2008) 87A (4), 980-985. *Bone regeneration in rabbit calvaria with novel monetite granules.*

22.- Faleh Tamimi, Jesus Torres, Isabel Tresguerres, Celia Clemente, Enrique Lopez Cabarcos, Luis Blanco Jerez. J. Clin. Periodontol. (2006) 33, 922-928. *Bone augmentation in rabbit calvariae: a comparative study between Bio-Oss$^{\rightarrow}$ and a novel ®-TCP/DCPD granulate.*

23-Racquel Zapanta LeGeros, Chem. Rev. (2008), 108, 4742–4753. *Calcium phosphate-based osteoconductive materials.*

24.- Gert W. Bos, , Ana Trullas-Jimeno, Wim Jiskoot, Daan J.A. Crommelin, Wim E. Hennink, Int. J. Pharmac. (2000) 211, 79–88, *Sterilization of poly(dimethylamino) ethyl methacrylate-based gene transfer complexes.*

25.- Ferry Verbaan, Inger van Dam, Yoshinubu Takakura, Mitsuru Hashida, Wim Hennink, Gert Storm, Christien Oussoren, Eur. J. Pharmac. Sci. (2003) 20, 419–427, *Intravenous fate of poly(2-(dimethylamino)ethyl methacrylate)- based polyplexes.*

26.- Mara Soares da Silva, Raquel Viveiros, Patricia I. Morgado, Ana Aguiar-Ricardo, Ilidio J. Correia, Teresa Casimiro, Int. J. Pharmac. (2011) 416, 61– 68, *Development of 2-(dimethylamino)ethyl methacrylate-based molecular recognition devices for controlled drug delivery using supercritical fluid technology.*

27.- Ferry J. Verbaan, Peter Klein Klouwenberg, Jan Hein van Steenis, Cor. J. Snel, Otto Boerman, Wim E. Hennink, Gert Storm, Int. J.Pharmac. (2005) 304, 185–192, *Application of poly(2-(dimethylamino)ethyl methacrylate)-based polyplexes for gene transfer into human ovarian carcinoma cells.*

28.- Ke Wang, Xu Xu, YuJun Wang, Xi Yan, Gang Guo, MeiJuan Huang, Feng Luo,Xia Zhao, YuQuan Wei, ZhiYong Qian, Int.J. Pharmac. (2010) 389, 130–138, *Synthesis and characterization of poly(methoxyl ethylene glycol-caprolactone-co-methacrylic acid-co-*

poly(ethylene glycol) methyl ether methacrylate) pH-sensitive hydrogel for delivery of dexamethasone.

29. – Henry V. K, David R. L, CRC Handbook of thermophysical and thermochemical data, CRC press Inc. 1994.

Table 1. Influence of the crosslinking content upon the various states of water in PEGMEM/DMAEM hydrogels.

Cross linking concentration	ESD	W_{∞} (%)	W_f (%)	W_{nf} (%)
0.25%	61.5	98.4	98.2	0.2
1%	38.9	97.5	96.3	1.2
2.5%	26.1	96.3	88.8	7.5
5%	19.3	95.0	80.6	14.4
10%	20.6	95.3	79.6	15.7
15%	5.2	83.9	67.9	16.0

Table.2. Values of d-spacing measured from SAED and those of Brushite Figure caption

Measured d –spacing (Å)	7.63	5.36	4.23	3.58	3.03
d-spacing of Brushite	7.59	5.24	4.24	3.62	3.06

Figures caption

Figure 1 Schematic representation of the diffusion of the electrolyte solutions from opposite ends within a gel (left side) and the corresponding set up of the experiment (right side).

Figure 2 Evolution of temperature during the gel formation as a function of initiator concentration.

Figure 3 ^{1}H NMR spectrum of the copolymer gel.

Figure 4 PEGMEM/DMAEM gels swelling (a) and deswelling (b) behaviour of PEGMEM/DMAEM gels as a function of crosslinker percentage and the ionic strength

Figure 5 DSC heating curve of PEGMEM/DMAEM gel prepared with (a) 25% cross linking agent and (b) with different crosslinking content. The corresponding enthalpy of Fusion (ΔH_{endo}) for each gel is given at the right side.

Figure 6 (a) Storage (G') and (b) Loss modulus (G") of gels with different concentration of crosslinker

● 1% ○ 2.5 % ▼ 5 % △ 7.5% ■ 15%

Figure 7 Series of pictures showing the formation of a band of precipitates as a function of time within a PEGMEM/DMAEM hydrogel prepared with 7% cross linking agent.

Figure 8 Position of the band of precipitates measured from edge through which flow the phosphate ions and also from the edge through which flow the calcium ions (a) Length of the gel and width of the band of precipitates (b) for PEGMEM/DMAEM hydrogels prepared with 2.5% and 7% cross linking content.

Figure 9 Micrograph of freeze dried 2.5 % cross-linked hydrogel at low magnification (x20).

Figure 10 Micrograph of the surface (left panel) and the inner part of the gels (right panel) as a function of the cross-linking content. The magnification was x5000 in all micrographs.

Figure 11 TEM pictures of the calcium phosphate microparticles.

Figure 12 Electron diffraction patterns of selected nanocrystals that, when aggregate, formed the round microparticles that can be seen with SEM.

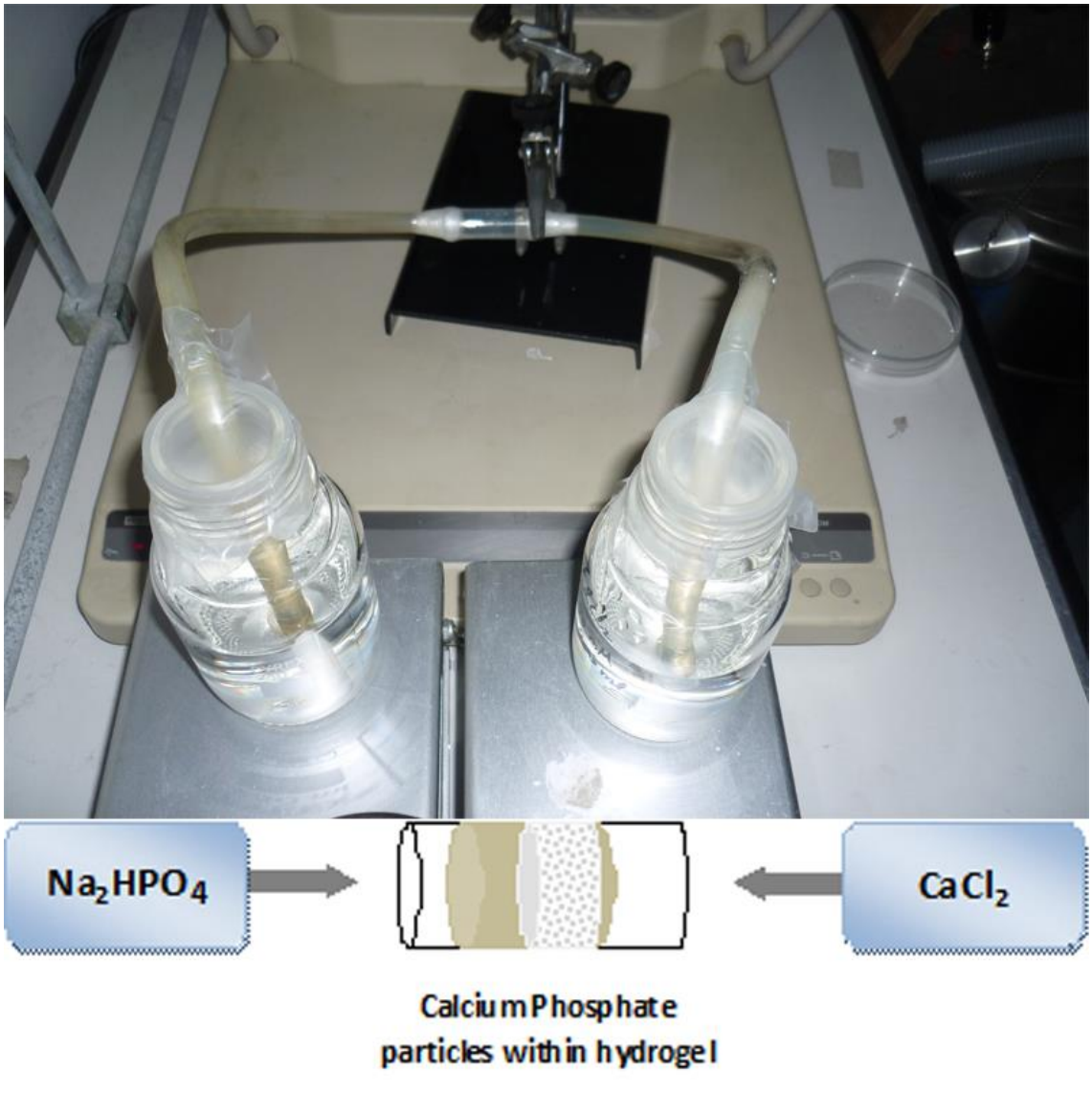
Na_2HPO_4
$CaCl_2$
Calcium Phosphate
particles within hydrogel

Figure 1

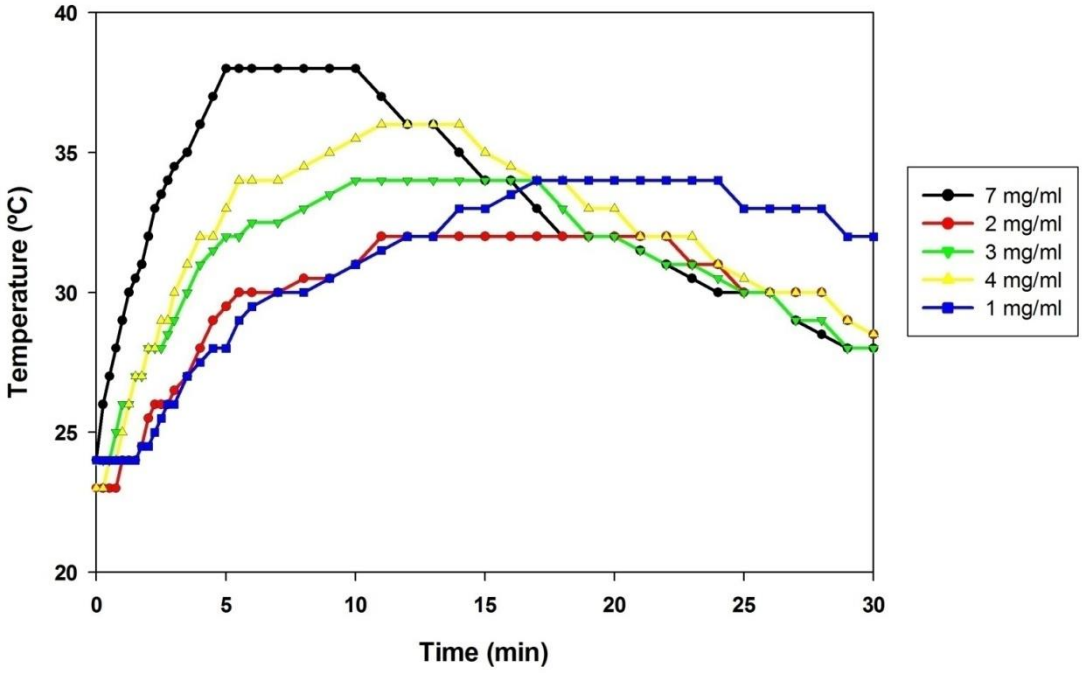
40
35
30
25
20
Temperature (ºC)
0
5
10
15
20
25
30
Time (min)
7 mg/ml
2 mg/ml
3 mg/ml
4 mg/ml
1 mg/ml

Figure 2

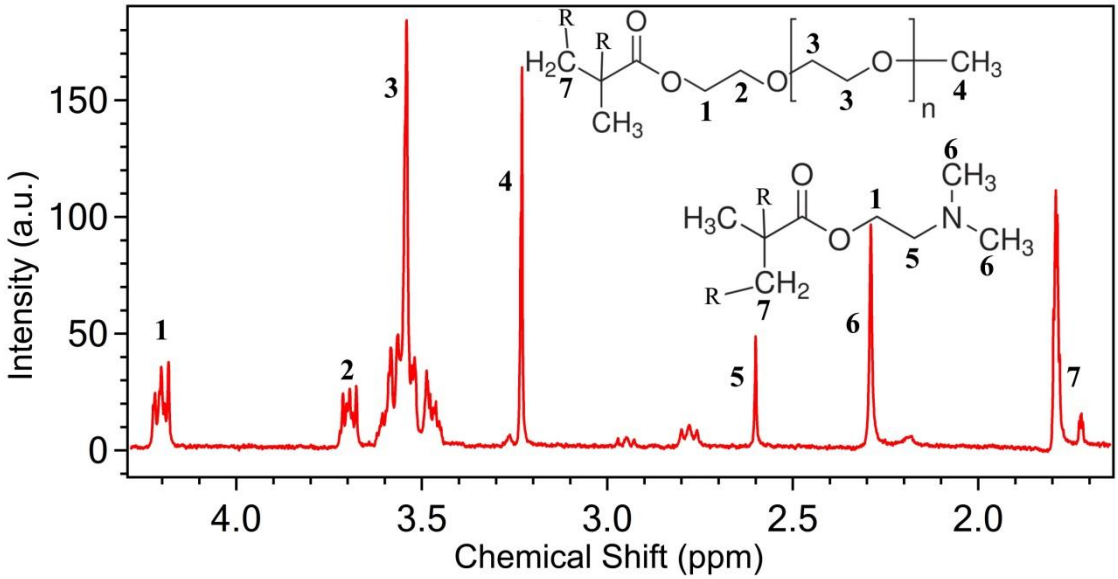
Intensity (a.u.)
150
100
50
0
4.0
3.5
3.0
2.5
2.0
Chemical Shift (ppm)
1
2
3
4
5
6
7
R
O
CH3
n

Figure 3

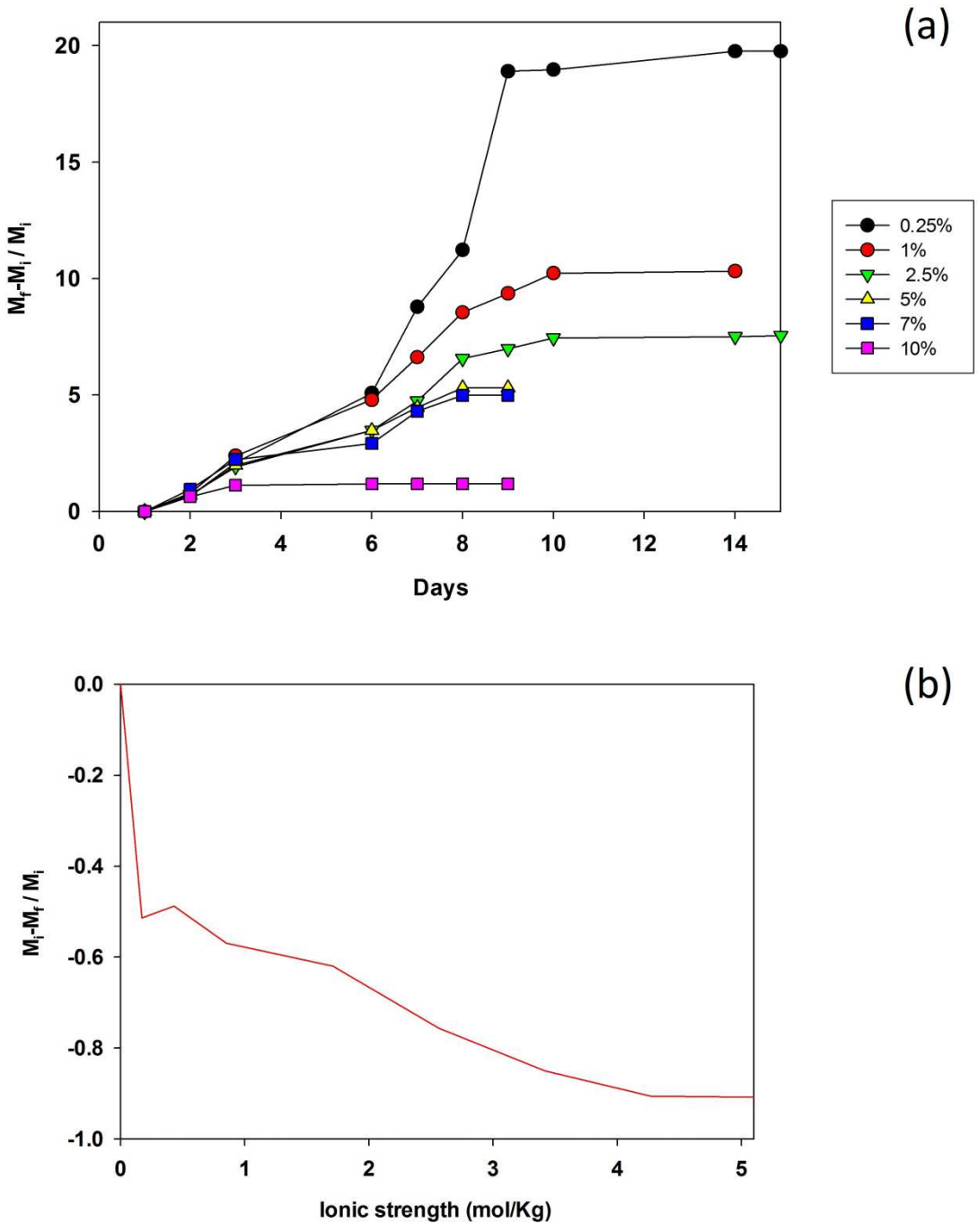
(a)
20
15
10
5
0
0
2
4
6
8
10
12
14
Days
M_f-M_i / M_i
0.25%
1%
2.5%
5%
7%
10%
(b)
0.0
-0.2
-0.4
-0.6
-0.8
-1.0
0
1
2
3
4
5
Ionic strength (mol/Kg)
M_i-M_f / M_i

Figure 4

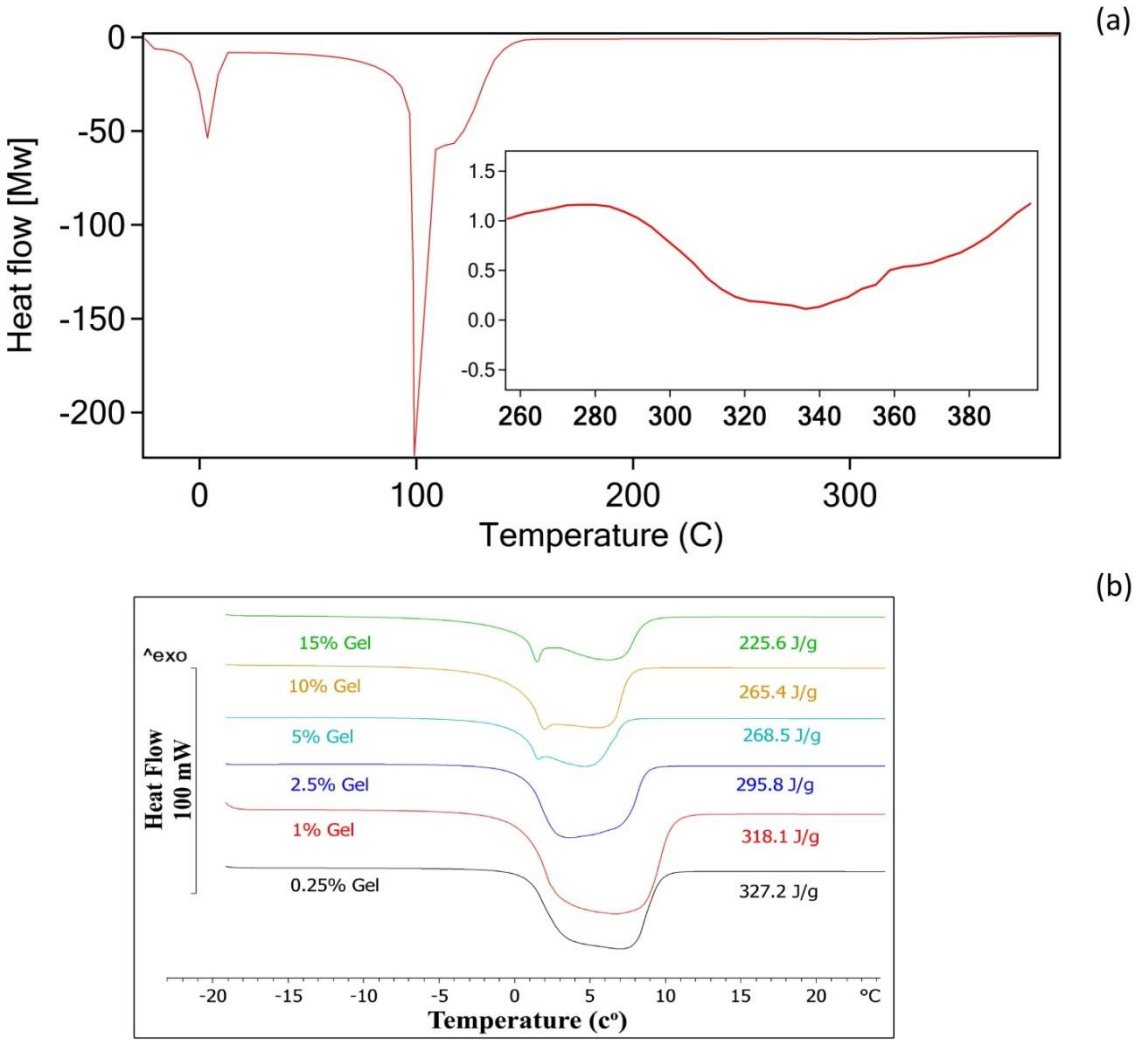
(a)
Heat flow [Mw]
0
-50
-100
-150
-200
0
100
200
300
Temperature (C)
1.5
1.0
0.5
0.0
-0.5
260
280
300
320
340
360
380
(b)
^exo
Heat Flow
100 mW
15% Gel
225.6 J/g
10% Gel
265.4 J/g
5% Gel
268.5 J/g
2.5% Gel
295.8 J/g
1% Gel
318.1 J/g
0.25% Gel
327.2 J/g
-20
-15
-10
-5
0
5
10
15
20
°C
Temperature (c°)

Figure 5

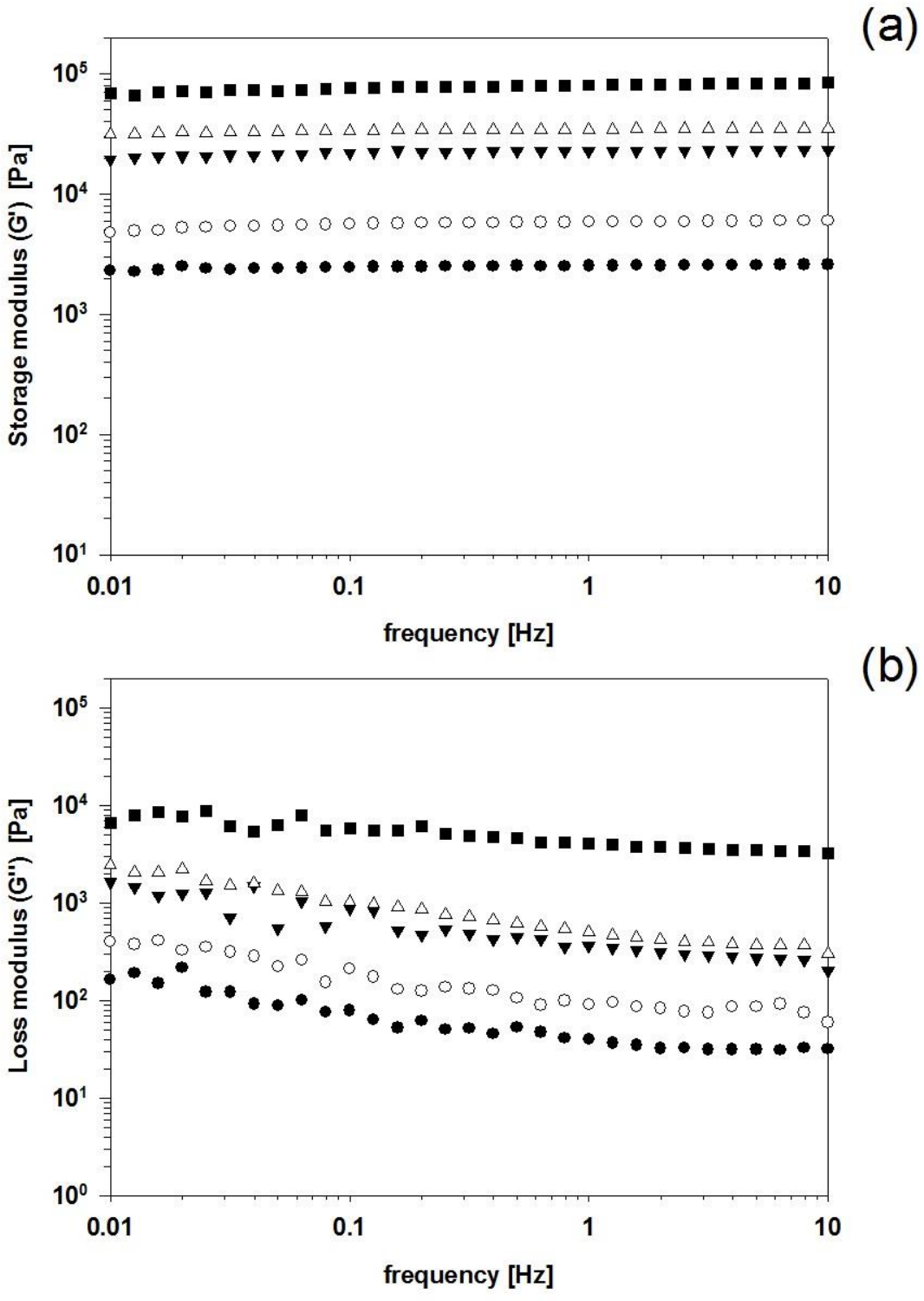
(a)
Storage modulus (G') [Pa]
10^5
10^4
10^3
10^2
10^1
0.01
0.1
1
10
frequency [Hz]
(b)
Loss modulus (G'') [Pa]
10^5
10^4
10^3
10^2
10^1
10^0
0.01
0.1
1
10
frequency [Hz]

Figure 6

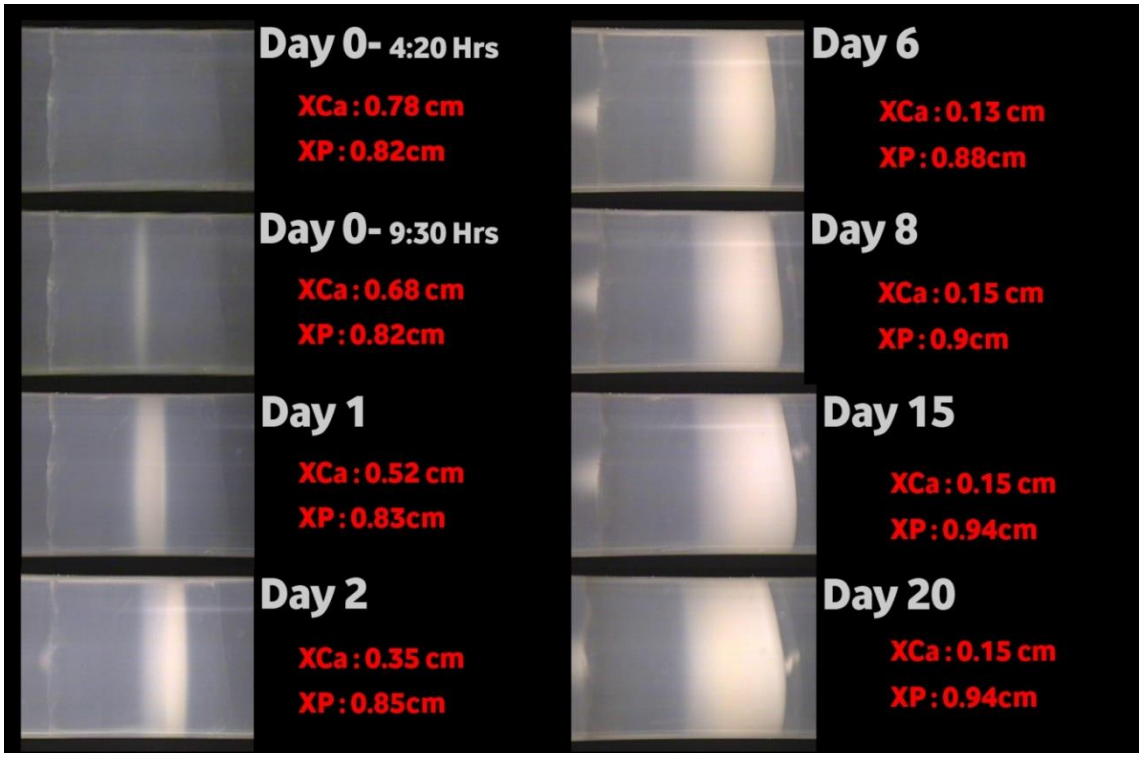
Day 0- 4:20 Hrs
XCa : 0.78 cm
XP : 0.82cm
Day 0- 9:30 Hrs
XCa : 0.68 cm
XP : 0.82cm
Day 1
XCa : 0.52 cm
XP : 0.83cm
Day 2
XCa : 0.35 cm
XP : 0.85cm
Day 6
XCa : 0.13 cm
XP : 0.88cm
Day 8
XCa : 0.15 cm
XP : 0.9cm
Day 15
XCa : 0.15 cm
XP : 0.94cm
Day 20
XCa : 0.15 cm
XP : 0.94cm

Figure 7

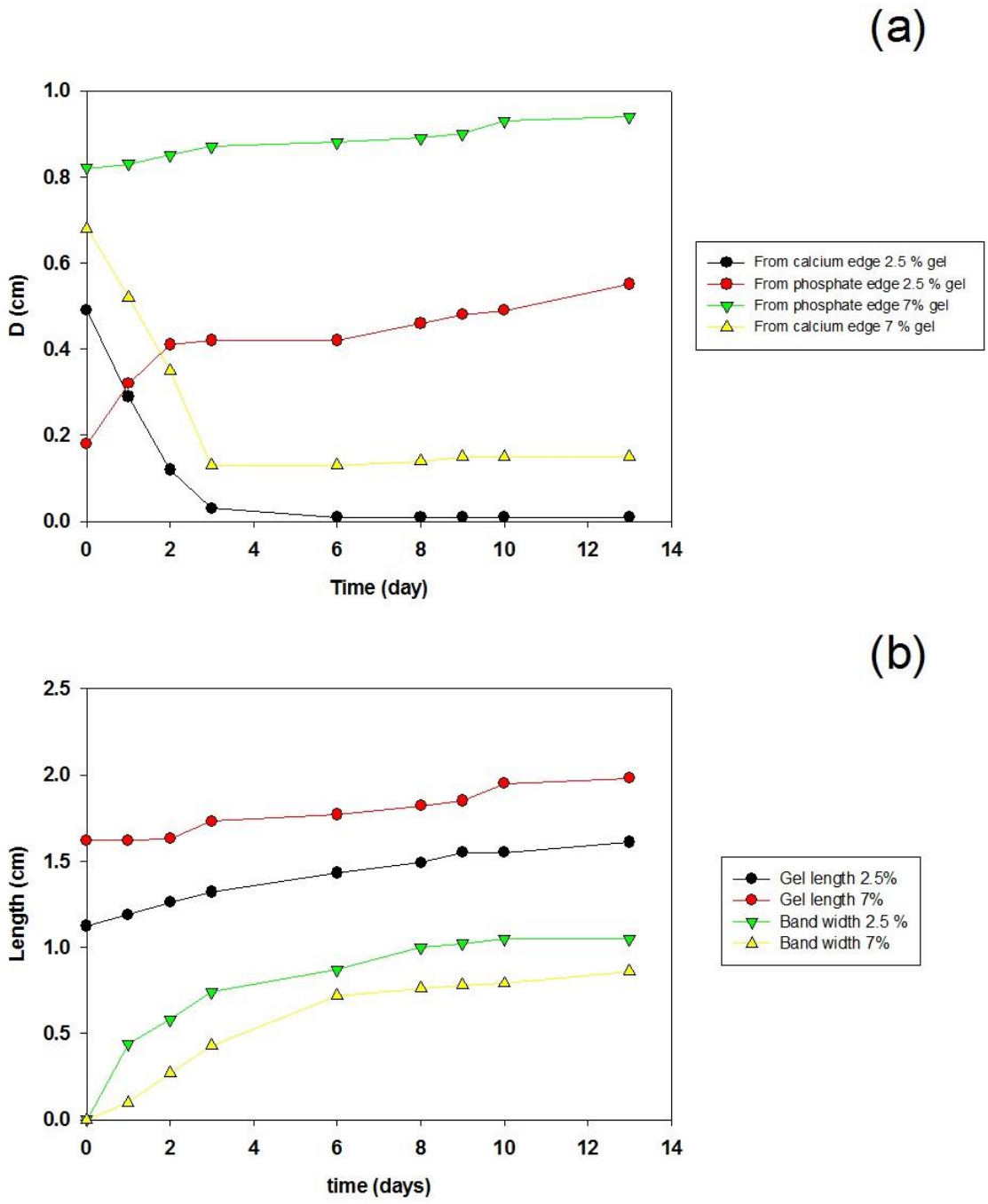
(a)
D (cm)
Time (day)
From calcium edge 2.5 % gel
From phosphate edge 2.5 % gel
From phosphate edge 7% gel
From calcium edge 7 % gel
(b)
Length (cm)
time (days)
Gel length 2.5%
Gel length 7%
Band width 2.5 %
Band width 7%

Figure 8

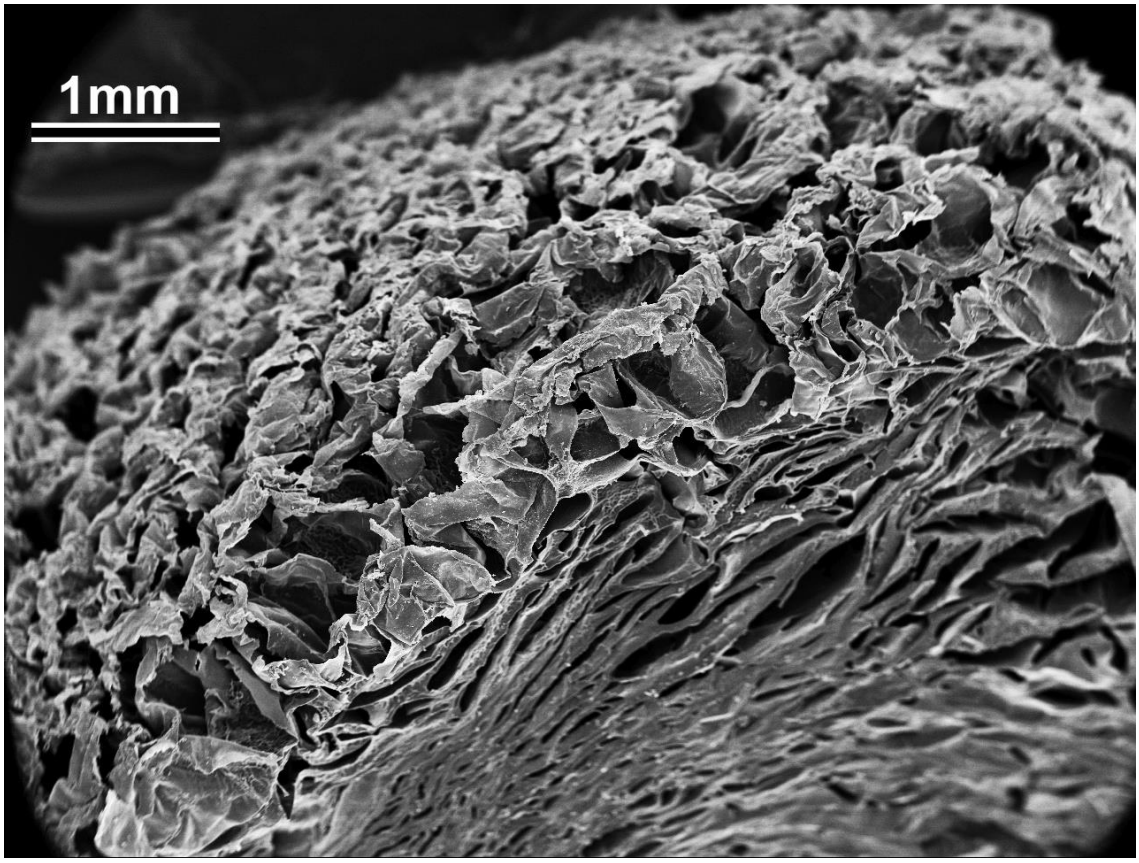

Figure 9

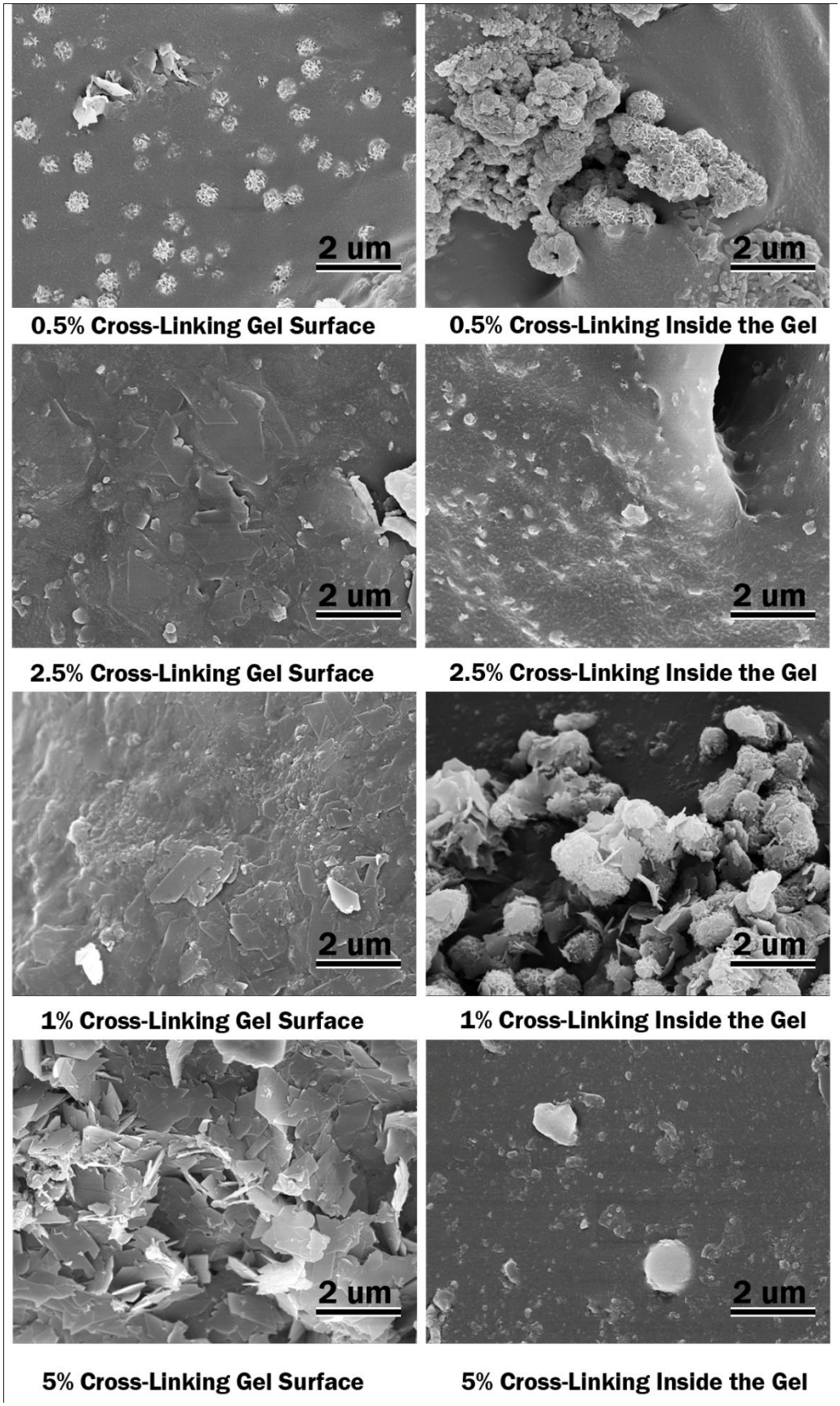
2 um
2 um
0.5% Cross-Linking Gel Surface
0.5% Cross-Linking Inside the Gel
2 um
2 um
2.5% Cross-Linking Gel Surface
2.5% Cross-Linking Inside the Gel
2 um
2 um
1% Cross-Linking Gel Surface
1% Cross-Linking Inside the Gel
2 um
2 um
5% Cross-Linking Gel Surface
5% Cross-Linking Inside the Gel

Figure 10

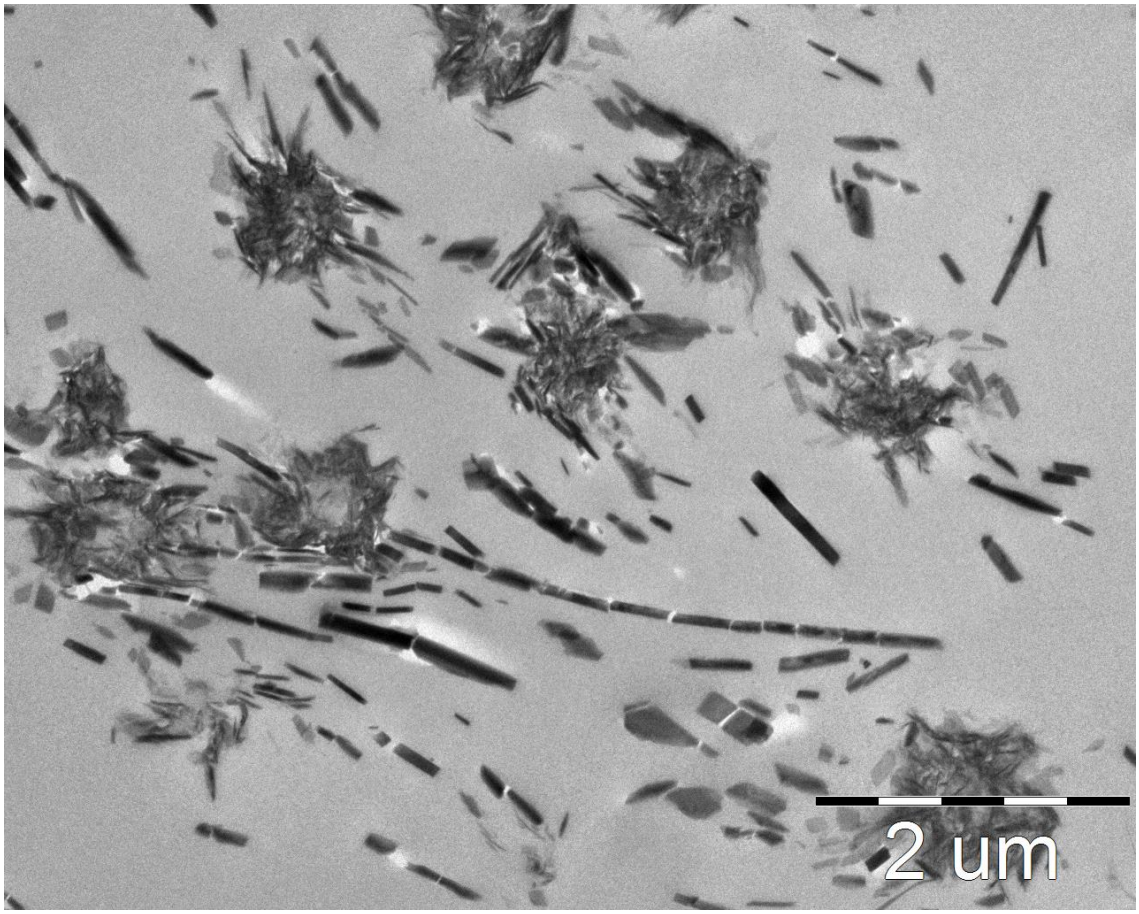

Figure 11

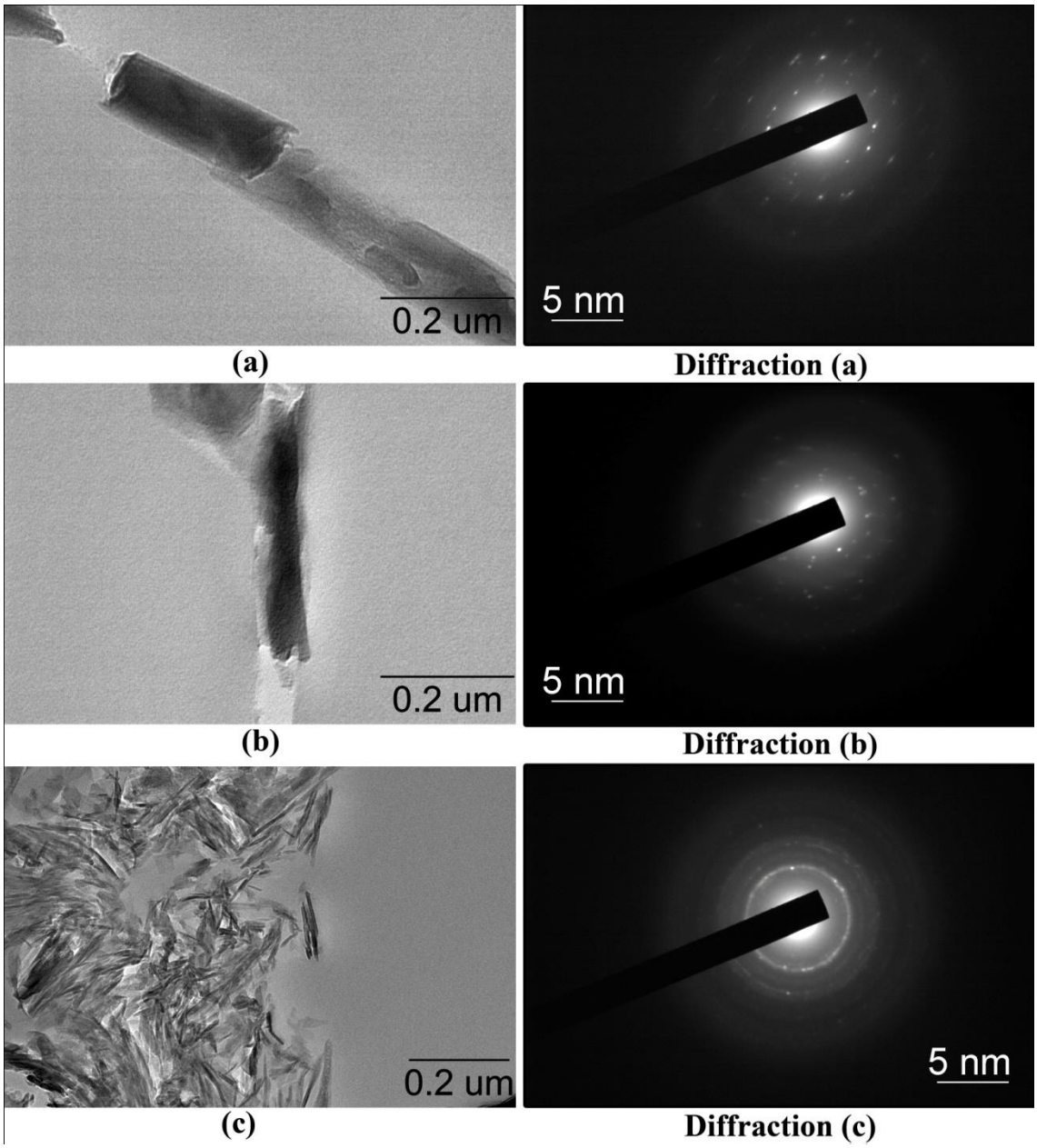
0.2 um
5 nm
(a)
Diffraction (a)
0.2 um
5 nm
(b)
Diffraction (b)
0.2 um
5 nm
(c)
Diffraction (c)

Figure 12